感度の高いウサギ P 抗体および免疫組織化学に汎用されている N 抗体を用いて狂犬病感染検体を抽出した。接種経路に関わらず、4 種類の抗体全てに対してマウスおよびサルの CNS で十分な染色性が認められた（表 2）（Figs. 1-4）。

Fig.1. No.25 (P-18 IC) 大脳基底核。

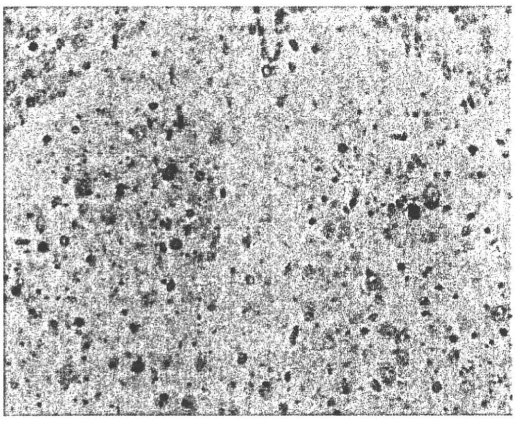

抗ウサギ P 抗体。神経細胞の細胞質に大小のスポット状の抗原陽性像が観察される。

Fig.2. No.20 (P-18 IC) 海馬。

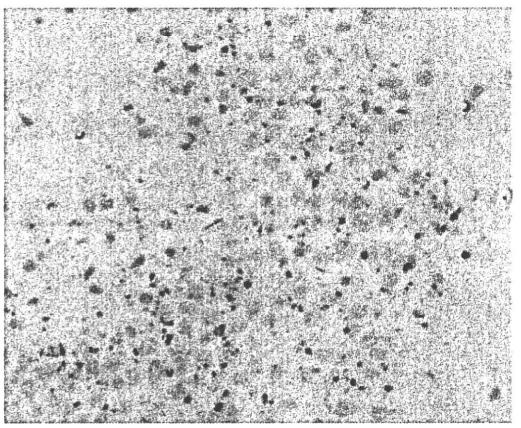

抗ウサギ N 抗体。海馬錐体細胞の細胞質に大小のスポット状の抗原陽性像が観察される。

Fig.3. No.25 (P-18 IC) 大脳基底核

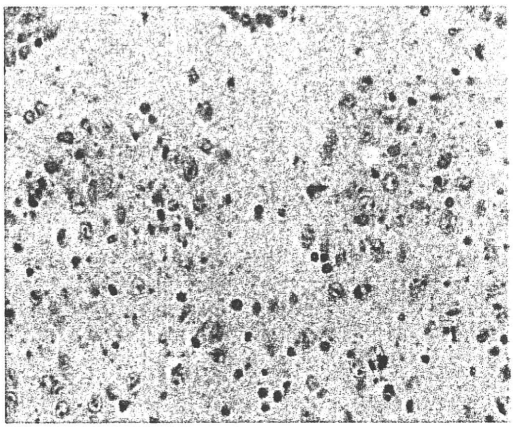

抗ニワトリ卵黄 P 抗体。神経細胞の細胞質に大小のスポット状の抗原陽性像が観察される。

Fig.4. No.20 (P-18 IC) 海馬。

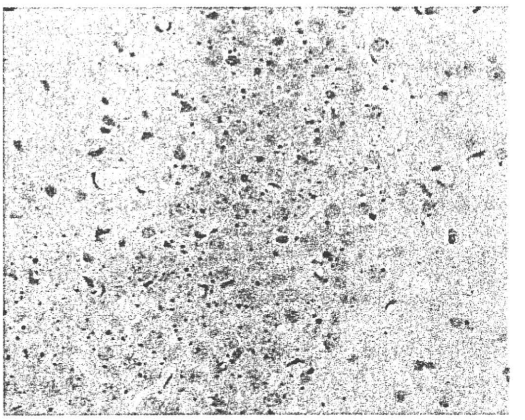

抗ニワトリ卵黄 N 抗体。神経細胞の細胞質に抗ウサギ N 抗体同様の抗原陽性像が観察される。

その中でニワトリ P 抗体は非特異反応が少なかった。ウイルス抗原は脊髄神経節を含む脊髄、延髄、中脳、小脳、大脳皮質、大脳基底核領域の神経細胞の細胞質内で瀰漫性に認められた。P-18 株および MP 株接種マウスの神経細胞では、概ねネグリ小体に一致して中型～大型のス

ポット状に染色される (Fig. 5) のに対し、CVS 株および P-17 株接種マウスの神経細胞では細顆粒状～小型のスポット状の陽性像が観察された (Fig. 6)。

Fig.5. No. 25 (P-18 IC) 延髄

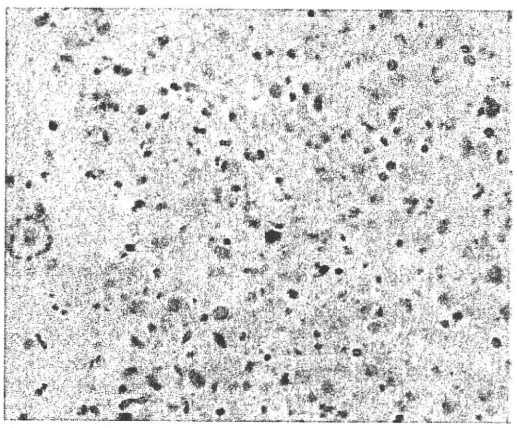

抗ウサギ N 抗体。ネグリ小体と概ね一致して中型～大型のスポット状の陽性像が観察される。

Fig.6. No. 10 (CVS-34 IC) 海馬。

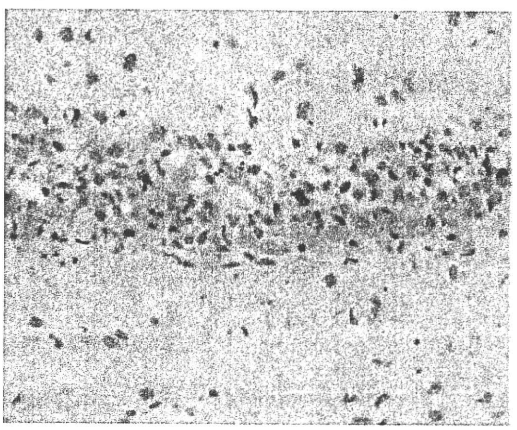

抗ニワトリ P 抗体。椎体層に細顆粒状～小型スポット状の陽性像が観察される。

また各蛋白抗体の染色性は、P 抗体を用いた場合では、感染細胞の細胞質のみならず、軸索、樹状突起において大小のスポット状に高率に観察された (Fig. 7) のに対し、N 抗体は主に神経細胞の細胞質にスポット状に検出され、軸索や樹状突起では P 抗体に比べわずかであった (Fig. 8)。

Fig.7. No. 33 (MP IM) 小脳脚。

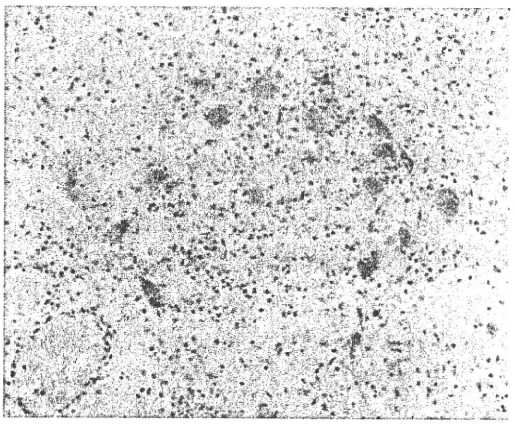

抗ウサギ P 抗体。抗体陽性像が細胞質のみならず、神経突起においても認められる。

Fig.8. No. 33 (MP IM) 小脳脚。

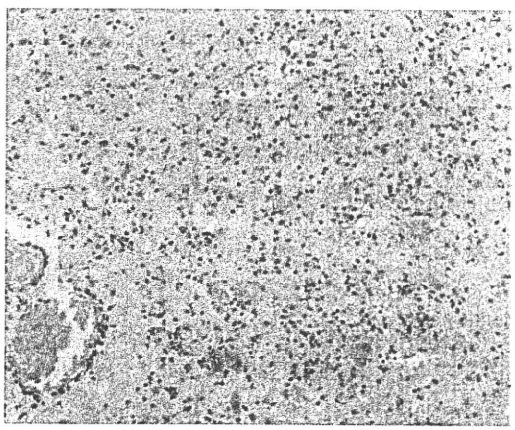

抗ウサギ N 抗体。P 抗体に比べて神経突起の陽性像は低い。

陽性神経細胞数は CVS 株接種マウスで

はN抗体に比較してP抗体において多数認められたが、野外株接種マウスではN抗体においてより多くの神経細胞が染色された。また、野外株（P-18、P-17、MP株）接種マウスでは接種経路に関係なくCVS株接種マウスに比較して小脳において陽性像が明らかに減少していた。

4. 超微形態学的所見

P-18株を接種したマウスの脊髄神経細胞の細胞質内に弾丸状および円形状の1層のエンベロープに被包された長さ約150nm、直径約70nmの成熟ウイルス粒子の集塊と電子密度の低い3～5μm大の大型類円形状のウイルス蛋白構造が観察された（Figs. 9, 10）。

Fig.9. P-18 (IM), 脊髄

脊髄神経細胞の細胞質に封入体（ネグリ小体，矢印）が観察される。

Fig.10. P-18 (IM), 脊髄

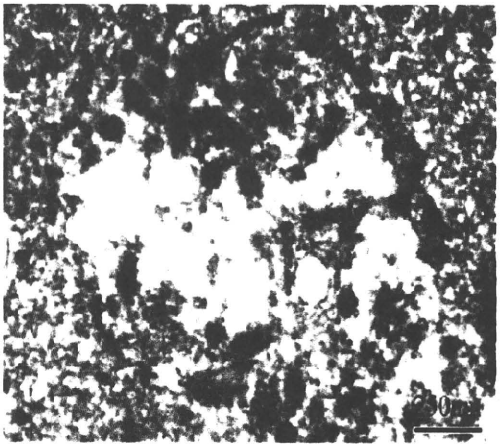

Fig.9の強拡大像。弾丸状および円形状の1層のエンベロープに被包された長さ約150nm，直径約70nmの成熟ウイルス粒子の集塊が観察される。

D. 考察

本研究では、狂犬病固定株 CVS-34 およびブラジルの吸血コウモリ、食虫コウモリ由来の狂犬病野外株をマウスに接種し、組織病変の違いを比較検討した。また、マウスとサルの中枢神経系を用いて、ニワトリ卵黄抗体の染色性についてウサギ血清と比較検討した。その結果、吸血コウモリ由来ウシ分離株、ヒツジ分離株および食虫コウモリ由来野外株の間には、マウスに対する組織病変が異なることが明らかになった。さらに、ニワトリ卵黄抗体をホルマリン固定後のパラフィンブロックに適用した場合、ウサギ抗体同様の染色感度が得られており、本抗体を用いた免疫組織化学的診断法の有用性が再確認された。

CVS 株をマウスやサルに接種した場合、接種経路に関係なく CNS のほぼ全域から検出される。しかし本実験では、P-17 株接種マウスの IC 群で、海馬錐体細胞、大脳において陽性細胞数は少なく、P-18 株および P-17 株接種マウスの IC 群においては小脳および小脳脚に陽性細胞が少ない傾向を示した。自然発生例のイヌでは、大脳や脳幹に比較して小脳では抗体陽性細胞が少ない。本実験に用いた翼手目由来の狂犬病ウイルスの体内移行様式や病原性については不明な点が多いが、動物種によって CNS におけるウイルス抗原の局在が多様であることを考慮すると、従来の海馬、脳幹、小脳を中心とした CNS の検索部位を再評価する必要があると思われる。

CVS 株をマウスやサルに接種した場合、自然発症例とは異なり光学顕微鏡レベルにおいてネグリ小体を見つけることは困難である。本研究では P-18 株および MP 株接種マウスの一部において、神経細胞の細胞質内にネグリ小体が観察された。自然発生例におけるネグリ小体の検出率は約 40～80%であり、株によっては観察されないこともある。本実験では、P-18 株を接種したマウスで 60%（9/15 例）、MP 株接種マウスでは 25%（4/16 例）の検出率であり、また P-17 株を接種したマウスの神経細胞では観察されなかった。P-18 株および P-17 株は同じく吸血コウモリ由来の分離株であるが、ネグリ小体の検出率に明らかな違いがみられることは興味深い所見である。その理由は不明であるが、吸血コウモリ由来のウイルスが次の宿主の体内で何回も継代される間にウイルスの増殖性や宿主に対する病原性が変化した可能性は否定できない。

ニワトリ P および N 抗体を用いた免疫組織化学的検索では、ウサギ抗体とほぼ同様の染色感度が得られた。特に、ニワトリ P 抗体はその他の抗体に比較して非特異反応がほとんど見られず、今後の病理診断に有効と思われた。抗体陽性像は P-18 株および MP 株を接種した一部のマウスでは、ネグリ小体が中～大型のスポ

ット状を呈したのに対し、P-17株およびCVS株を接種したマウスでは比較的小型なスポット状の陽性像を示した。一般的にウイルス抗原の組織学的検出には、凍結生材料かホルマリン固定パラフィン材料を利用している。凍結生材料と比較してホルマリン固定パラフィン材料は感染性がなく、長期保存が可能であり、特別な装置を必要としないため安全かつ安価で確定診断が可能である。本実験に用いたウサギ抗体を 1.4g 作製するためには、成ウサギ 1 羽が必要なのに対し、ニワトリ抗体は卵 14 個で十分である。従って、ニワトリ抗体を用いた免疫組織化学的診断は安全で安価な確定診断が期待できる。今後は今回確立した免疫染色の手法を自然感染例に応用し、各種抗体の染色感度について更に比較検討すべきであると思われる。

E.　結論

本研究では、まず、吸血コウモリ由来のヒツジ分離株（P-18 株）、ウシ分離株（P-17 株）および食虫コウモリ分離株（MP 株）をマウスの筋肉内および脳内に接種し、CNS における病理組織学的変化を株間で比較した。次に、ニワトリ卵黄抗体をこれらの野外株とサルの組織に適用し、免疫組織化学的診断系の確立を試みた。

その結果、P-18 株と MP 株を接種したマウスでは、光学顕微鏡レベルにおいて脊髄神経節、脊髄、延髄、中脳、海馬および大脳皮質に小型から大型なネグリ小体が多数観察されたが、P-17 ではいずれの部位においても認められなかった。

ニワトリ卵黄由来のＮおよびＰ抗体を用いた免疫染色では、接種経路や動物種に関わらずウサギ由来のＮおよびＰ抗体と同程度の染色感度が認められた。従って、今後自然発症例においても十分応用できると思われた。

F.　健康危機情報

特になし

G.　研究発表

1　論文発表

(1) Kojima D, Park CH, Tsujikawa S, Kohara K, Hatai H, Oyamada T, Noguchi A, Inoue S. Lesions of the Central Nervous System Induced by Intracerebral Inoculation of BALB/c Mice with Rabies Virus (CVS-11). *J. Vet. Med. Sci.* 72(8):1011-1016.

2　口頭発表

(1) 小嶋　大亮, 朴　天鎬, 石田　誠, 小原　慶子, 井上　謙一, 畑井　仁, 小山田敏文, 井上 智. 狂犬病ウイルス固定株(CVS-11)を脳内接種した Macaque 属サルの脳に関する病理学的研究. 第 150 回日本獣医学会学術集会講演要旨集 p. 176. 2010. 9. 18, 帯広畜産大学

H.　知的財産権の出願・登録状況

1　特許取得　なし

2　その他　なし

FULL PAPER *Pathology*

Lesions of the Central Nervous System Induced by Intracerebral Inoculation of BALB/c Mice with Rabies Virus (CVS-11)

Daisuke KOJIMA[1], Chun-Ho PARK[1]*, Shintarou TSUJIKAWA[1], Keiko KOHARA[1], Hitoshi HATAI[1], Toshifumi OYAMADA[1], Akira NOGUCHI[2] and Satoshi INOUE[2]

[1]*Department of Veterinary Pathology, School of Veterinary Medicine, Kitasato University, 23–35–1 Higashi, Towada, Aomori 034–8628 and* [2]*Department of Veterinary Science, National Institute of Infectious Diseases, 1–23–1 Toyama, Shinjuku-ku, Tokyo, 162–8640 Japan*

(Received 8 December 2009/Accepted 10 March 2010/Published online in J-STAGE 25 March 2010)

ABSTRACT. BALB/c mice were inoculated intracerebrally with fixed rabies virus (CVS-11) and pathomorphological changes in the central nervous system were studied. Infected mice showed ruffled hair, hunchback, anorexia, emaciation and ataxia at 5 days postinoculation (DPI), but paralysis did not occur. Viral antigens were first detected in the pyramidal cells of the cerebral cortex and hippocampus at 3 DPI, and these cells exhibited apoptosis at 5 DPI. Microglial cells and astroglial cells significantly increased in the areas of the nerve cells which showed apoptosis. However, spinal neurons and spinal dorsal root ganglion cells did not exhibit apoptosis despite virus infection. These observations indicate that different mechanism which causes apoptosis exists among the neurons of the brain and spinal cord, and glial cells play an important role in pathogenesis of the experimental rabies.

KEY WORDS: BALB/c mice, intracerebral inoculation, pathogenesis, rabies virus (CVS-11).

J. Vet. Med. Sci. 72(8): 1011–1016, 2010

Rabies is an ancient disease that is still endemic in many parts of the world and is a serious public health problem in developing countries, especially in Asia. Approximately 55,000 human deaths are caused by rabies each year [9, 10]. An understanding of the pathogenesis of rabies is important for developing novel therapies and preventive measures for rabies, which may be fatal for humans and animals.

Previously, we demonstrated that C57BL/6J mice inoculated intramuscularly with CVS-11 showed paralysis with severe spinal lesions [15]. The spinal lesions were composed of the infiltration of T lymphocytes, the increase of microglial cells and astroglial cells and the majority of T lymphocytes exhibited apoptosis. In contrast, marked neuronal apoptosis was detected in the cerebral cortex, hippocampus and cerebellum of mice that were inoculated intracerebrally with CVS-11, but paralysis was absent [21]. Induction of apoptosis by fixed strain of rabies virus has been reported *in vitro* [19] and experimental animal models [11, 13] to be associated with the expression level of the virus protein. On the other hand, the street strain of human [12] and silver-haired bat rabies virus [27] does not induce apoptosis in the brain. These observations indicate that the various strains of rabies viruses are susceptible to nervous cells, but different mechanisms exist to induce neurological diseases. The apparent differences in the pathology observed in various animals could result from differences in the pathogenicity of the different strains of rabies, their modes of infection, the immune status of the hosts, and the varying susceptibility of the rabies. Currently it remains unclear which factors are responsible for differences in clinical symptoms and the roles of non-neuron cells specially glial cells in the central nervous system (CNS) after rabies virus infection are not fully investigated.

To obtain the more information about pathogenesis of rabies in mice, CVS-11 was inoculated into the cerebrum of BALB/c mice and the target cells of apoptosis and the kinetics of glial cells in the CNS were studied during the infection.

MATERIALS AND METHODS

Virus, mice and viral inoculation: The CVS-11 strain of fixed rabies virus, which was obtained from Dr. C. E. Rupprecht (Rabies Section, Virus and Rickettsia Zoonoses Branch, Centers for Disease Control and Preservation, Atlanta, GA, U.S.A.), was grown in mouse A/J (H-2a) neuroblastoma cells as previously described [24]. Twenty-four 6-week-old female BALB/c mice were purchased from Japan SLC, Inc. (Shizuoka, Japan). Twenty-one mice were inoculated intracerebrally (right frontal lobe of the cerebrum) with viral doses of 10^5 plaque-forming units of the CVS-11 strain suspended in phosphate-buffered saline (PBS, pH 7.4) and three uninfected control mice were inoculated with PBS alone. The inoculated mice were observed daily for neurological symptoms and were killed at 2, 3, 4, 5, 7, 10 and 11 DPI (three mice per day). All experiments were performed in level-2 biosafety laboratories according to the Committee on Biosafety and Animal Handling and Ethical Regulation of the National Institute of Infectious Diseases, Japan. Animal care, breeding, virus inoculation and observation were performed in accordance with the guidelines of the committee.

Necropsy and preparation of tissue sections: Each mouse was anesthetized with chloroform and perfused transcar-

* CORRESPONDENCE TO: PARK, C.-H., Department of Veterinary Pathology, School of Veterinary Medicine, Kitasato University, 23–35–1 Higashi, Towada, Aomori 034–8628, Japan.
e-mail: baku@vmas.kitasato-u.ac.jp

dially with 10–15 m*l* of PBS followed by freshly prepared 4% paraformaldehyde in 0.1 M PBS. Spinal samples were removed and fixed in 4% paraformaldehyde at room temperature (RT) for less than 24 hr and were decalcified in K-CX solution (Fujisawa Pharmaceutical Co., Ltd., Osaka, Japan). Transverse sections of spinal cords at the cervical (C3–4), thoracic (T1–3), lumbar (L1–2) and sacral (S1–3) vertebrae were prepared. A complete series of paraffin sections about 3 μm thick was cut and mounted on glass slides. Serial sections were subjected to hematoxylin and eosin (HE) staining, immunohistochemistry and *in situ* terminal deoxynucleotidyl transferase-mediated deoxyuridine triphosphate (dUTP) nick end labeling (TUNEL).

Immunohistochemistry: For detection of rabies virus antigens in tissues, all sections were stained using the streptavidin-biotin-peroxidase complex method using anti-rabbit phosphoprotein (P) [15]. For detection of cell type, the following primary antibodies were used: anti-glial fibrillary acidic protein (GFAP) for astroglial cells (Nichirei Biosciences, Tokyo, Japan); anti-ionized calcium binding adaptor molecule 1 (Iba1) for microglial cells (Wako, Osaka, Japan); anti-CD3 for T lymphocytes (DAKO, Kyoto, Japan); and anti-CD20 for B lymphocytes (Spring Bioscience, Fremont, CA, U.S.A.). Briefly, tissue sections were treated with 0.25% trypsin (for P) at RT for 30 min, with 750 W microwaves (for CD3 and CD20) for 5 min or in a water bath (for Iba1) at 95°C for 15 min.

To remove endogenous peroxidase, immunostained sections were treated with 0.3% H_2O_2 in methanol (for P) or 3% H_2O_2 in methanol (for GFAP, Iba1, CD3 and CD20). To block nonspecific reactions, each immunostained section was treated with 5% normal goat serum (for P) or 10% normal goat serum (for GFAP, Iba1, CD3 and CD20). Primary antibodies were diluted in PBS (1:1000 for P and 1:500 for Iba1) and incubated at 4°C overnight. Antibodies against GFAP, CD3 and CD20 were incubated at RT for 1 hr. Anti-rabbit IgG (Nichirei) was used as a secondary antibody for immunostaining for P and Iba1. The Envision + System Labeled Polymer-HRP anti-rabbit antibody (DAKO) was used for immunostaining for CD3 and CD20. Histofine® Simple Stain MAX-PO (Nichirei) was used for immunostaining for GFAP. Finally, each antibody was visualized using 3-3'-diaminobenzidine (DAB, DAKO). Slides were counterstained with hematoxylin.

TUNEL assays: The presence of fragmented DNA was evaluated using TUNEL (Chemicon, Temecula, CA, U.S.A.). After deparaffinizing the sections, endogenous peroxidase activity was removed by exposure to 0.3% H_2O_2 in methanol for 30 min at RT. Then, sections were treated with 20 mg/m*l* proteinase-K in 0.1 M PBS (DAKO) for 15 min at RT to retrieve antigens. After washing in PBS, sections were prepared according to the manufacturer's instructions and were counterstained with hematoxylin.

Double labeling with TUNEL and immunostaining: Double labeling of a single tissue section was used for analysis of apoptosis and the coexpression of antigens. Firstly, TUNEL assays were performed and slides were incubated with DAB until color developed. The reaction was stopped by washing the slides in distilled water, and then antibodies against P, CD3, Iba1 or GFAP were added. Histofine® Simple Stain AP (Rabbit) (Nichirei) was used as a secondary antibody. The color reaction was developed using Histofine® New Fuchsin (Nichirei). The slides were counterstained with hematoxylin.

Counting of TUNEL-positive and immunostained cells in the cerebrum and cervical spinal cord: All TUNEL-positive cells and cells immunostained for P, Iba1, GFAP and CD3 in the cerebrum (cerebral cortex, thalamus and hippocampus) and cervical spinal cord, including the dorsal root spinal ganglion, were counted using a light microscope with a magnification of × 100–200 on 3, 5 and 10 DPI (three mice per day).

RESULTS

Clinical signs and macroscopic findings: Mice showed ruffled hair, hunched backs, anorexia, emaciation and ataxia at 5 DPI and became moribund at 8 DPI. All mice died by 11 DPI, and no mice showed paralysis before death. No macroscopic findings were observed at necropsy.

Histology: Nuclear pyknosis and fragmentation and cytoplasmic shrinkage were first observed in the pyramidal cells (CA3) of the hippocampus at 4 DPI, and most of the pyramidal cells had been destroyed by 7 DPI (Fig. 1). Lesser changes were observed in the neurons of the cerebral cortex pyramidal cells, thalamus neurons, cerebellum Purkinje cells and cerebellum granule cells. Nuclear pyknosis and cytoplasmic shrinkage were detected in the dorsal root spinal ganglion cells at 5 DPI (Fig. 2). No histological changes were observed in the spinal neurons.

On the other hand, mild inflammatory cells composed mainly of lymphocytes were observed around the small vessels and cerebral ventricles and under the leptomeninges, and large activated microglial cells were observed throughout the CNS at 5 DPI. More advanced lesions appeared at 7 DPI, and the majority of lymphocytes showed nuclear fragmentation and pyknosis.

Immunohistochemistry: Virus antigens were first detected as small spots in the pyramidal cells of the cerebral cortex and hippocampus at 3 DPI and in the cerebellum Purkinje cells, neurons of the thalamus, brain stem, spinal cord (C, T, L, S) and dorsal root spinal ganglion at 5 DPI. As infection progressed, virus antigens were also detected in the dendrites and axons of neurons.

At 2 DPI, rod-like small microglial cells were scattered throughout the brain and spinal cord. From 3 to 5 DPI, the number of microglial cells increased and their morphology changed from rod to ramified or amoeboid (Fig. 3). These morphological changes were more evident in the cerebral cortex, hippocampus and brain stem than in the spinal cord. Astroglial cells were scattered throughout the parenchyma, under the leptomeninges, around the small vessels and the central canal of the brain and spinal cord at 3 DPI. From 5 DPI, astroglial cells were activated in the brain and their

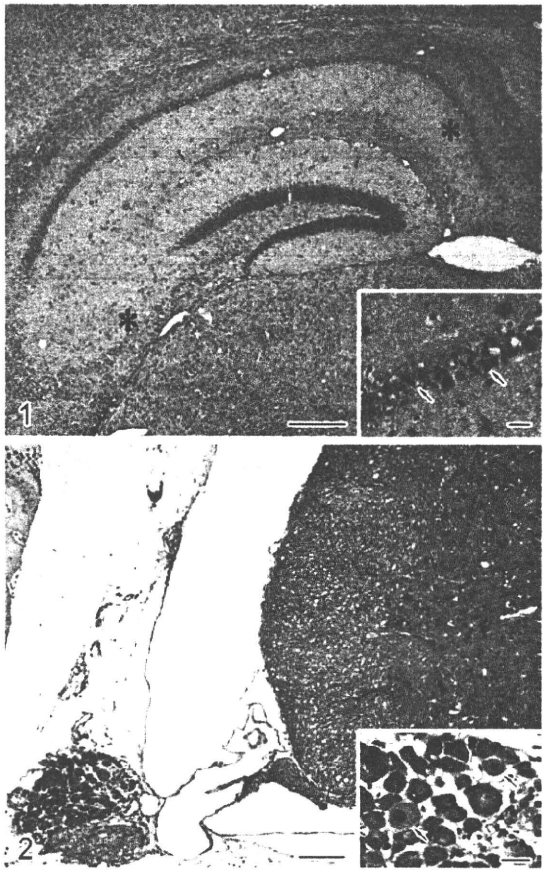

Fig. 1. Hippocampus. Necrotic changes (*) in the CA 1 and CA 3 regions of the pyramidal layer are evident. Nuclear pyknosis and fragmentation and cytoplasmic shrinkage are evident in the pyramidal cells 7 DPI (arrows, inset). HE. Bars=250 μm and 25 μm (inset).

Fig. 2. Lumber spinal ganglion. There are no morphological changes in the spinal cord. Nuclear pyknosis and cytoplasmic shrinkage are observed in the dorsal root spinal ganglion cells (arrows, inset) 5 DPI. HE. Bars=100 μm and 25 μm (inset).

morphology changed. The processes of fibrous astroglial cells elongated from the leptomeninges to the deep parenchyma and many large protoplasmic astroglial cells were detected simultaneously in the parenchyma of the brain (Fig. 4), particularly around apoptotic neurons. There were no significant changes of astroglial cells in the spinal cord throughout the experimental period.

At 5 DPI, CD3-positive T lymphocytes appeared under the leptomeninges and around the blood vessels and ventricles of the entire CNS, but the extent of infiltration of T lymphocytes became greater in the brain than in the spinal cord as the infection progressed. On the other hand, CD20-positive B lymphocytes were not detected in the CNS throughout the experimental period. The mean of the number of glial cells around apoptotic neurons and lymphocytes in multiple areas (cerebral cortex, thalamus, hippocampus) of brain and cervical spinal cords at time course was summarized in Table 1.

TUNEL assays and double staining: At 5 DPI, TUNEL positive nerve cells appeared in the cerebral cortex pyramidal cells, thalamus neurons, hippocampus pyramidal cells, cerebellum Purkinje cells and cerebellum granule layer cells, and those of TUNEL positive neurons were significantly increased at 10 DPI, particularly in the pyramidal cells of the hippocampus (Table 2 and Fig. 5). On the other hand, TUNEL positive signal was not detected in the spinal neurons, including the dorsal root spinal ganglion cells (Table 2). The majority of microglial cells and astroglial cells were TUNEL negative. Double staining confirmed that all apoptotic neurons, except for the cerebellum granule layer cells, were infected with CVS-11 (Fig. 6). T lymphocytes that exhibited nuclear fragmentation and pyknosis by HE staining were TUNEL positive.

DISCUSSION

In this study, BALB/c mice that were inoculated intracerebrally with CVS-11 did not exhibit paralytic signs and the pathological changes were mainly located in the cerebral cortex, hippocampus, thalamus neurons, cerebellum Purkinje cells and cerebellum granule layer cells and were accompanied by inflammation. In addition, the majority of virus-infected neurons of the brain and T lymphocytes underwent apoptosis, but spinal lesions were mild and apoptotic features were not observed in the virus-infected spinal neurons or dorsal root spinal ganglion cells. These findings differ substantially from those of mice that were inoculated intramuscularly [15]. Guigoni and Coulon [6] reported that in primary cultures of CVS-infected pyramidal cells of the hippocampus, more than 90% of cells showed apoptosis within 3 DPI, whereas the rat spinal motor neurons did not show major evidence of apoptosis over a period of 7 DPI. In addition, primary dorsal root spinal ganglion cells show long term survival up to 4 weeks when they are chronically infected in cell culture with rabies virus [16]. Our previous report and those of others suggest that various types of neurons are susceptible to CVS-11 [6, 15], and different mechanism which causes apoptosis exists among the neurons of the brain and spinal cord.

In this study, the inflammatory cells in the brain consisted mainly of T lymphocytes and microglial cells; their numbers increased as infection progressed and most T lymphocytes in the brain and spinal cord underwent apoptosis. These results correspond with those for mice that were inoculated with CVS-11 intramuscularly [15]. Infection of experimental animals with an attenuated strain of the rabies virus induces a strong specific immune response that results in a nonlethal infection, whereas mice that were infected using salivary glands from a naturally infected dog showed severe suppression of immunity caused by lymphocyte apoptosis [14, 25]. In addition, Iwasaki *et al.* [8] reported that immunocompetent mice show severe paralytic disease and

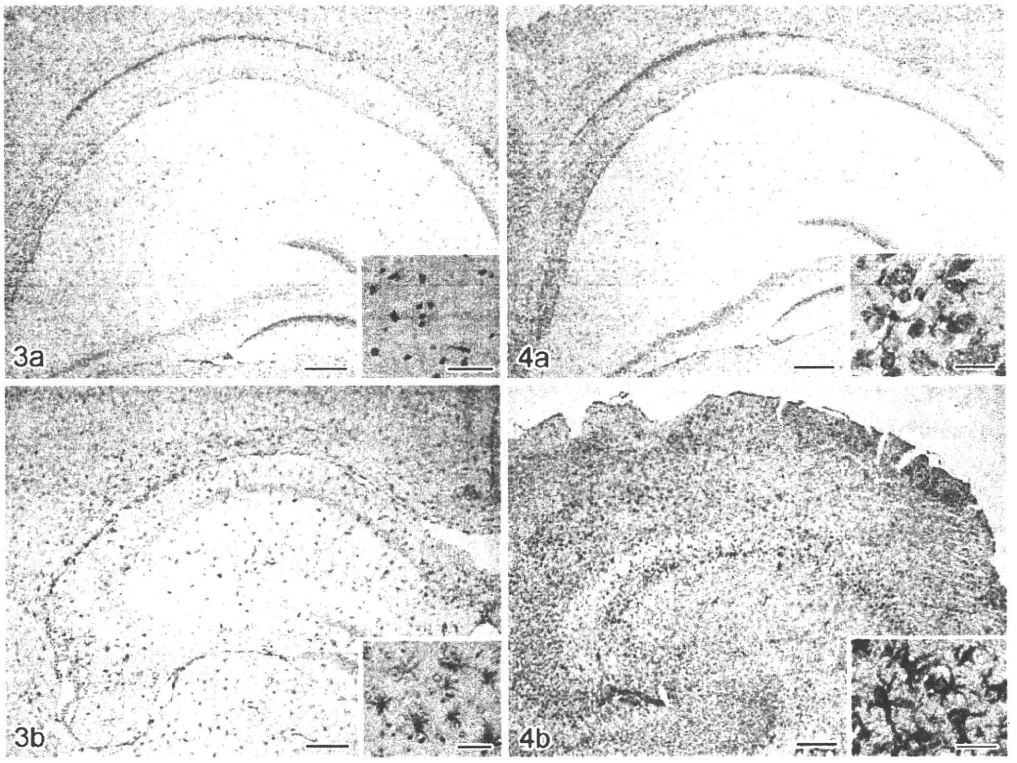

Fig. 3. Hippocampus. There are no morphological changes (a) and small rod-like microglial cells are observed 2 DPI (a, inset). In contrast, an increase in the number of microglial cells with a ramified or amoeboid shape (b, inset) was observed 5 DPI. Immunohistochemistry (anti-Iba1). Bars=250 μm and 50 μm (inset).

Fig. 4. Hippocampus. There are no morphological changes (a) and few astroglial cells 3 DPI (a, inset). In contrast, an increased number of astroglial cells (b) of protoplasmic shape are observed 5 DPI (b, inset). Immunohistochemistry (anti-GFAP). Bars=250 μm and 25 μm (inset).

Table 1. The mean of the number of glial cells and lymphocytes in three mice infected with CVS-11

Cerebral cortex, thalamus and hippocampus	3 DPI (n=3)	5 DPI (n=3)	10 DPI (n=3)
GFAP	67	272	454
Iba1	974	1,732	2,045
CD3	0	76	294
CD20	0	0	0
Cervical spinal cord/ spinal ganglion			
GFAP	16/0	15/0	21/0
Iba1	37/0	124/0	148/0
CD3	0/0	17/15	45/32
CD20	0/0	0/0	0/0

GFAP: astroglial cell (protoplasmic astrogliall cells type only counted), Iba1: microglial cell (ramified or amoeboid microglial cells type only counted), CD3: T lymphocyte, CD20: B lymphocyte.

marked inflammation and degeneration of the CNS. In contrast, immunosuppressed mice developed encephalitic symptoms with only minor paralysis. Individual neuronal degeneration and microglial reaction were mild even though the level of antirabies antibody was similar to that of immunocompetent mice. These findings suggest that T lymphocyte immune reactions play a role in the pathogenesis of rabies. In the present study, the reasons of apoptosis of lymphocytes were not investigated, but currently it is suggested that T lymphocyte mediated Fas/Fas ligand pathways

Table 2. The mean of the number of TUNEL positive neurons in three mice infected with CVS-11

Nerve cells in the brain and spinal cord	3 DPI (n=3)	5 DPI (n=3)	10 DPI (n=3)
Cerebral cortex pyramidal cells	0	47	326
Thalamus neurons	0	52	257
Hippocampus pyramidal cells	0	72	463
Cerebllum Purkinje cells	0	8	15
Cerebllum granule layer cells	0	16	62
Cervical spinal neurons	0	0	0
Cervical dorsal root ganglion cells	0	0	0

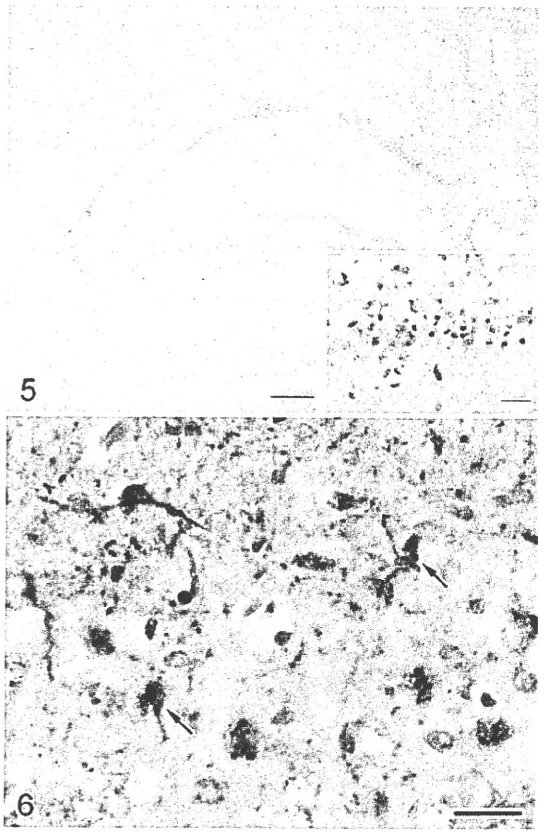

Fig. 5. Hippocampus. Marked staining is evident in pyramidal neurons, but not in the neurons of the dentate gyrus. Most pyramidal cells shows morphological changes characteristic of apoptosis 7 DPI (inset). TUNEL assay. Bars=250 μm and 25 μm (inset).

Fig. 6. Cerebral cortex. Pyramidal neurons (arrows) stained positively with TUNEL (brown) and anti-P antibody (red) 7 DPI. TUNEL assay and Immunohistochemistry. Bar=30 μm.

expressed within infected neurons and lymphocytes apoptosis [2].

In the present study, the number of microglial cells positive to anti-Iba1 antibody increased significantly at 3 DPI and their morphological features changed to a ramified or amoeboid form in areas of apoptosis. Those findings were more significant in the brains than spinal cords throughout the experimental period. Activated microglial cells release proinflammatory cytokines such as interleukin (IL)-1 [5], tumor necrosis factor (TNF)-α [22, 26] and nitric oxide (NO) [18], which cause neuronal cell death both directly and indirectly via the induction of NO and free radicals [7, 23]. IL-1 and TNF-α are released by microglial cells and macrophages, and play an important role in coordinating the inflammatory response associated with rabies encephalopathy [3, 17].

Astroglial cells provide structural, metabolic and trophic support for neurons. As might be expected from their wide range of activities, both beneficial and detrimental effects are attributed to activated astroglial cells [1, 4, 20]. In a previous study in which mice were inoculated with CVS-11 intramuscularly, we observed that numerous spinal neurons underwent necrosis and that the number of astroglial cells increased as the infection progressed [15]. In the present study, the reaction of astroglial cells was mild and there were no morphological changes in the spinal cord despite infection of many spinal and spinal ganglion neurons. Therefore, it was suggested that the number of astroglial cells increased in response to neuronal cell death by apoptosis.

In the present study, most pathomorphological changes after intracerebral inoculation are located in the brain, and spinal lesions are slight compared with those of intramuscularly infected mice. These findings suggest that expression of a paralytic symptom in rabies infection in mice is determined by differences in the route of inoculation. In addition, increasing of glial cells is essential features of CVS-11 infection in mice, this process may also play an important role in pathogenesis of experimental rabies.

ACKNOWLEDGMENTS. This work was supported by a Grant-in-Aid for Scientific Research from the Japanese Society for the Promotion of science (grant No. 6604–19380171–0044) and was partly supported by a Research on Emerging and Reemerging Infectious Disease Grant from the Ministry of Health, Labour and Welfare of Japan.

REFERENCES

1. Aschner, M. 1998. Astrocytes as mediators of immune and

inflammatory responses in the CNS. *Neurotoxicology* **19**: 269–282.
2. Baloul, L., Camelo, S. and Lafon, M. 2004. Up-regulation of Fas ligand (FasL) in the central nervous system: a mechanism of immune evasion by rabies virus. *J. Neurovirol.* **10**: 372–382.
3. Camelo, S., Castellanos, J., Lafage, M. and Lafon, M. 2001. Rabies virus ocular disease: T-cell-dependent protection is under the control of signaling by the p55 tumor necrosis factor alpha receptor, p55TNFR. *J. Virol.* **75**: 3427–3434.
4. Faulkner, J. R., Herrmann, J. E., Woo, M. J., Tansey, K. E., Doan, N. B. and Sofroniew, M. V. 2004. Reactive astrocytes protect tissue and preserve function after spinal cord injury. *J. Neurosci.* **24**: 2143–2155.
5. Giulian, D., Baker, T. J., Shih, L. C. and Lachman, L. B. 1986. Interleukin 1 of the central nervous system is produced by ameboid microglia. *J. Exp. Med.* **164**: 594–604.
6. Guigoni, C. and Coulon, P. 2002. Rabies virus is not cytolytic for rat spinal motoneurons *in vitro*. *J. Neurovirol.* **8**: 306–317.
7. Hu, S., Peterson, P. K. and Chao, C. C. 1997. Cytokine-mediated neuronal apoptosis. *Neurochem. Int.* **30**: 427–431.
8. Iwasaki, Y., Gerhard, W. and Clark, H. F. 1977. Role of host immune response in the development of either encephalitic or paralytic disease after experimental rabies infection in mice. *Infect. Immun.* **18**: 220–225.
9. Jackson, A. C. 2002. Human disease. pp. 123–180. *In*: Rabies 2nd ed. (Jackson A. C. and Wunner W. H. eds.), Academic Press, London.
10. Jackson, A. C. 2002. Update on rabies. *Curr. Opin. Neurol.* **15**: 327–331.
11. Jackson, A. C. and Park, H. 1998. Apoptotic cell death in experimental rabies in suckling mice. *Acta Neuropathol.* **95**: 159–164.
12. Jackson, A. C., Randle, E., Lawrance, G. and Rossiter, J. P. 2008. Neuronal apoptosis does not play an important role in human rabies encephalitis. *J. Neurovirol.* **14**: 368–375.
13. Jackson, A. C. and Rossiter, J. P. 1997. Apoptosis plays an important role in experimental rabies virus infection. *J. Virol.* **71**: 5603–5607.
14. Kasempimolporn, S., Tirawatnapong, T., Saengseesom, W., Nookhai, S. and Sitprija, V. 2001. Immunosuppression in rabies virus infection mediated by lymphocyte apoptosis. *Jpn. J. Infect. Dis.* **54**: 144–147.
15. Kojima, D., Park, C. H., Satoh, Y., Inoue, S., Noguchi, A., Yamada, A. and Oyamada, T. 2009. Pathology of the spinal cord of C57BL/6J mice infected with rabies virus (CVS-11). *J. Vet. Med. Sci.* **71**: 319–324.
16. Lycke, E. and Tsiang, H. 1987. Rabies virus infection of cultured rat sensory neurons. *J. Virol.* **61**: 2733–2741.
17. Marquette, C., Van Dam, A. M., Ceccaldi, P. E., Weber, P., Haour, F. and Tsiang, H. 1996. Induction of immunoreactive interleukin-1 beta and tumor necrosis factor-alpha in the brains of rabies virus infected rats. *J. Neuroimmunol.* **68**: 45–51.
18. Meda, L., Cassatella, M. A., Szendrei, G. I., Otvos, Jr. L., Baron, P., Villalba, M., Ferrari, D. and Rossl, F. 1995. Activation of microglial cells by beta-amyloid protein and interferon-gamma. *Nature* **374**: 647–650.
19. Morimoto, K., Hooper, D. C., Spitsin, S., Koprowski, H. and Dietzschold, B. 1999. Pathogenicity of different rabies virus variants inversely correlates with apoptosis and rabies virus glycoprotein expression in infected primary neuron cultures. *J. Virol.* **73**: 510–518.
20. Myer, D. J., Gurkoff, G. G., Lee, S. M., Hovda, D. A. and Sofroniew, M. V. 2006. Essential protective roles of reactive astrocytes in traumatic brain injury. *Brain* **129**: 2761–2772.
21. Park, C. H., Kondo, M., Inoue, S., Noguchi, A., Oyamada, T., Yoshikawa, H. and Yamada, A. 2006. The histopathogenesis of paralytic rabies in six-week-old C57BL/6J mice following inoculation of the CVS-11 strain into the right triceps surae muscle. *J. Vet. Med. Sci.* **68**: 589–595.
22. Sawada, M., Kondo, N., Suzumura, A. and Marunouchi, T. 1989. Production of tumor necrosis factor-alpha by microglia and astrocytes in culture. *Brain Res.* **491**: 394–397.
23. Selmaj, K., Raine, C. S. and Cross, A. H. 1991. Anti-tumor necrosis factor therapy abrogates autoimmune demyelination. *Ann. Neurol.* **30**: 694–700.
24. Smith, J. S., Yager, P. A. and Baer, G. M. 1996. A rapid tissue culture test for determining rabies-neutralizing antibody. pp. 371–373. *In*: Laboratory Techniques in Rabies, 4th ed. (Meslin, F.X., Kaplan, M. M. and Koprowski, H. eds.), World Health Organization, Geneva.
25. Wiktor, T. J., Doherty, P. C. and Koprowski, H. 1977. *In vitro* evidence of cell-mediated immunity after exposure of mice to both live and inactivated rabies virus. *Proc. Natl. Acad. Sci. U.S.A.* **74**: 334–338.
26. Wood, P. L. 1995. Microglia as a unique cellular target in the treatment of stroke: potential neurotoxic mediators produced by activated microglia. *Neurol. Res.* **17**: 242–248.
27. Yan, X., Prosniak, M., Curtis, M, T., Weiss, M., L., Faber, M., Dietzschold, B. and Fu, Z. F. 2001. Silver-haired bat rabies virus variant does not induce apoptosis in the brain of experimentally infected mice. *J. Neurovirol.* **7**: 518–527.

Summary of the cooperation project to evaluate the RFFIT, to extend and apply RFFIT in rabies surveillance supported by NIID grant in 2010

Name of researcher in China; Peng-Cheng Yu (1), Xin-Jun Lv(1), Xin-Xin Shen (1), Hao Li (1), Li-Hua Wang (1), Xue-Chun Zhang (2), Gui-Hua Huang (3),Qing Tang (1), and Guo-Dong Liang (1)

Affiliation;

(1)Department of Viral Encephalitis, Institute for Viral Disease Control and Prevention, China CDC, Beijing, China;

(2)Beijing Center for Disease Control and Prevention, Beijing, China;

(3)Guangzhou Center for Disease Control and Prevention, Guangzhou, China.

Correspondence: Qing Tang, Phone number: 86-10-63539777 or 58900895; Fax:86-10-58900895; Email:qtang04@sina.com

The rapid fluorescent focus inhibition test (RFFIT) is one of the methods recommended by WHO to detect the rabies neutralization antibody for rabies patients and post exposure prophylaxes. RFFIT has internalized by our nation dispensatory as the standard specification test to detect the rabies neutralization antibody from 2010. RFFIT can be used in the people's determination of rabies neutralizing antibodies and can also be used in animals. The establishment of RFFIT test can improve the rabies laboratory detection ability and will enhance the overall surveillance system of rabies in China.

The establishment of the rapid fluorescent focus inhibition test (RFFIT)

BSR cells were cultured in large quantities and frozen in low temperature for establishing the BSR cell bank. Detecting the CVS-11 seed virus titer by DFA up to 1.7×107 FFU/ml, CVS-11 seed virus was adapted to BSR cells(80%

infection with CVS-11, Fig 1) to prepare 500 ampoules of titrated CVS-11 stock virus which was frozen in -80℃.

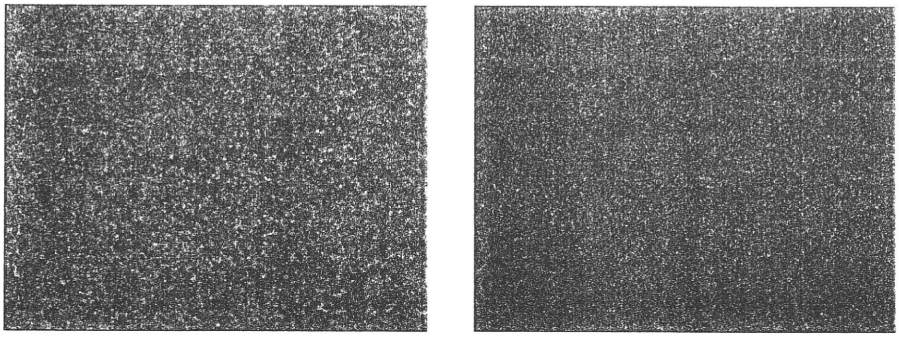

80% infection of BSR cell with CVS-11 BSR cell control

Fig.1 CVS-11 80% infection of BSR cell and BSR cell control

Detecting the CVS-11stock virus titer by DFA up to 2×10^7 FFU/ml, the best challenging dose of the CVS-11 stock virus is 6×10^6 FFU/ml, which would be used in the RFFIT test.

According the protocol of the RFFIT test used in the Institute Pasteur in France, to set the virus control, cell control, standard serum control, negative serum control, strong positive serum control and the weak positive serum control in the RFFIT system, and developed the calculation formula based on the Reed & Muench method formulas and Microsoft Excel software, which can calculate the serum titers simply.

To detect a large number of serum use the RFFIT test, the results indicated that the specificity of the RFFIT is 100% and the stability is very good which showed that the RFFIT system can be used in the detection of rabies neutralization antibody.

Comparison of the WHO Standard Rabies Immunoglobulin and the National Standard Human Rabies Immunoglobulin Used in the RFFIT in China.

Setting the WHO standard immunoglobulin(SHRCW) and the national standard immunoglobulin(SHRCC) in the same RFFIT system and testing 12 human serum at the same time, compare the fluorescence percentage of the

two different standard immunoglobulin through the 12 serum testing results using the calculation formula of neutralization antibody titer(Tab.1).

Tab.1 Comparison of the titer calculated from WHO and China standard immunoglobulin

Sample	Antibody titer		Sample	Antibody titer		Sample	Antibody titer	
	SHRCW	SHRCC		SHRCW	SHRCC		SHRCW	SHRCC
SHRFO	9.01	6.12	**3**	2.53	1.55	**8**	3.65	2.23
SHRFA	1.06	0.65	**4**	19.71	12.06	**LH**	5.03	3.08
SHRN	—	—	**5**	25.41	15.51	**HY**	3.92	2.40
1	3.95	2.42	**6**	4.63	2.83	**XQ**	10.41	6.37
2	18.55	11.35	**7**	5.06	3.10	**A7**	288.69	139.88

The results showed that the 50% percent fluorescence of the two standard immunoglobulin are all between the fifth and sixth wells(Fig 2), the fluorescence percentage of the national standard immunoglobulin is lower than the WHO standard immunoglobulin. The test result for the same serum calculated from the WHO standard immunoglobulin is a little higher than that of the national standard immunoglobulin, which tell us there is difference between the two standard immunoglobulin, but it is not influence the evaluation of the serum neutralization antibody titer.

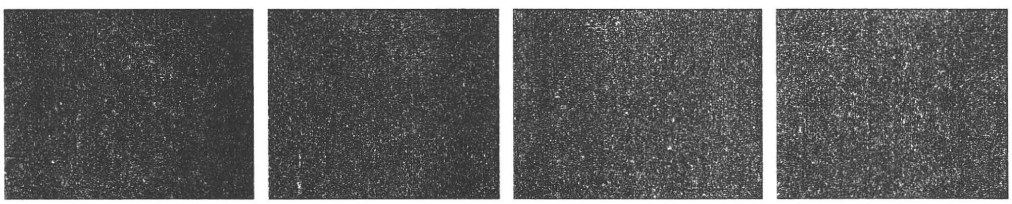

C D E F

Fig 2. Comparison of 50% infective dose between WHO and China standard immunoglobulin

C: is the 30% infective dose in the WHO standard immunoglobulin in the fifth well

D: is the 70% infective dose in the WHO standard immunoglobulin in the sixth well

E: is the 18% infective dose in the national standard immunoglobulin in the fifth well

F: is the 68% infective dose in the national standard immunoglobulin in the sixth well

RFFIT in rabies surveillance

The RFFIT method established in our lab has very high consistency with that

from other domestic laboratories when parallel compared. Then the established RFFIT system was applied to detect the specimens sent from other province or city CDCs or some research projects, the results showed that viral neutralizing antibodies against rabies virus were generated on Day 7 following immunization with the majority of domestic rabies vaccines, and reached 100% seroconversion rates on Day 14 to Day 45, and maintained above 90% after one year post-immunization. Preliminary applications suggest that this detection system has good performance in the aspects of specificity, sensitivity, stability and repeatability. It can be applied not only for assessment of the viral neutralizing antibodies level against rabies virus, but also for laboratory-based diagnosis, titer determination of immune preparations and effectiveness evaluation for new vaccines or new immunization procedures. This detection system can improve the overall surveillance capacity of rabies in China.

The work of communication and cooperation on RFFIT between the scientists from the both of NIID and Institute for Viral Disease Control and Prevention of China CDC in Japan, 5-19 Dec 2010

December 5-19, 2010, Miss Peng-cheng Yu from Institute for Viral Disease Control and Prevention China CDC goes to the Department of Veterinary Science, National Institute of Infectious Diseases(NIID) in Japan for the communication and cooperation work supported by the NIID foundation in Japan for the cooperation project to evaluate the rapid fluorescent inhibition test RFFIT, to extend and apply RFFIT in rabies surveillance between the Institute for Viral Disease Control and Prevention China CDC and NIID Japan. The Standard Rabies Immunoglobulin used in NIID Japan is 2IU/ml potency, prepared by NIID. Miss Peng-cheng Yu brings another two Standard Rabies Immunoglobulin used in the Institute for Viral Disease Control and Prevention of China CDC, which include the WHO Standard Rabies Immunoglobulin and the China National Standard Human Rabies Immunoglobulin. The potency of

WHO Standard Rabies Immunoglobulin is 3O IU/ml; the potency of Chinese National Standard Human Rabies Immunoglobulin is 21.4IU/ml.

(1)RFFIT detection system used in NIID in Japan

To detect the four serum samples with the RFFIT detection system of NIID in Japan parallel using the different Standard Rabies Immunoglobulin by both of Miss Peng-cheng Yu and Mr. Noguchi, the detection result shows in Table 2.

Table2. Serum detection using RFFIT system of NIID Japan, Yu & Noguchi

Sample & Standard Immunoglobulin	Primitive titer of serum	2010.12.07data			
		NIID-RFFIT			
		Noguchi observation		Yu observation	
		Noguchi plate	Yu plate	Noguchi plate	Yu plate
WHO	30	46.03	46.69	46.77	54.73
China	21.4	39.54	38.70	39.35	46.54
Ar-1	10.1	10.22	9.79	10.25	11.15
Ar-2	6.13	NT	NT	NT	NT
Sa-1	5.21	NT	NT	NT	NT
Sa-2	2.09	2.09	2.04	2.20	2.53
SI(x100) 0.5IU/ml	0.41	0.42	0.39	0.45	0.37
Negateive	<0.02	NT	NT	NT	NT
SI(x25) 2IU/ml	2.00	2.00	2.00	2.00	2.00

Result explanation:

a)The detected titer of the WHO Standard Rabies Immunoglobulin and the Chinese Standard Human Rabies Immunoglobulin is much higher than their Primitive titer, there is a significant difference. The detection result shows that there existed the big difference between the Standard Rabies Immunoglobulin of NIID Japan and the WHO Standard Rabies Immunoglobulin and the Chinese Standard Human Rabies Immunoglobulin used in the Institute for Viral Disease Control and Prevention of China CDC.

b)For the same serum sample, the primitive titer was determined by the Standard Rabies Immunoglobulin of NIID, such as the primitive titer was 0.41IU/ml based on 0.5IU/ml Standard Immunoglobulin diluted from the Standard Rabies Immunoglobulin of NIID. To detect this serum no matter by

Miss Peng-cheng Yu or by Mr. Noguchi, there is the difference compared their detection results with the primitive titer, but the difference is not significant.

(2)RFFIT detection system used in Viral Disease Control and Prevention China CDC

To detect the same four serum samples using the RFFIT detection system of Viral Disease Control and Prevention in China CDC parallel with the different Standard Rabies Immunoglobulin by both of Miss Peng-cheng Yu and Mr. Noguchi, the detection result shows in Table 3.

Table 3. Serum detection using RFFIT system of Viral Disease Control and Prevention China CDC, Noguchi, Yu & Inoue

Sample & Standard Immunoglobulin	Primitive titer serum		2010.12.10data		
			China-RFFIT (Yu Plate)		
			observation		
			Noguchi	Yu	Inoue
WHO	30		31.18	54.00	41.03
China	21.4		31.18	48.00	41.03
Ar-1	10.1		7.21	12.17	9.48
Ar-2	6.13		6.00	7.43	7.90
Sa-1	5.21		5.38	6.00	4.56
Sa-2	2.09		2.47	4.04	3.16
SI(x100) 0.5IU/ml	0.41		0.60	0.46	0.42
Negateive	<0.02		<0.08	<0.11	<0.11
SI(x25) 2IU/ml	2.00		2.00	2.00	2.00

Result explanation:

a)The Standard Rabies Immunoglobulin of NIID Japan was used to detected titer of the WHO Standard Rabies Immunoglobulin and the Chinese Standard Human Rabies Immunoglobulin by the RFFIT detection system of Viral Disease Control and Prevention China CDC, the detected titer is much higher than their primitive titer, there is significant difference.

b)For the same 0.5IU/ml serum sample in the RFFIT detection system of Viral Disease Control and Prevention, judging the result by the different scientists, the detection result also showed the difference.

c)The judging result in the RFFIT detection system of Viral Disease Control and Prevention is according to the percentage of the fluorescence, but the judging in NIID is differed from this, which might be the reason of difference in judging RFFIT result between the two labs.

(3)Repeat the detection of RFFIT using the detection system of Viral Disease Control and Prevention China CDC

To detect the same four serum samples again with the Standard Rabies Immunoglobulin of NIID Japan using the RFFIT detection system of Viral Disease Control and Prevention China CDC, the detection result is as showing in Table 4:

Table 4. Repeat the serum detection using the RFFIT detection system of Viral Disease Control and Prevention China CDC

Sample & Standard Immunoglobulin	Primitive titer of serum		2010.12.15data			
			China-RFFIT			
			Noguchi observation		Yu observation	
			Noguchi plate	Yu plate	Noguchi plate	Yu plate
WHO	30		44.96	46.49	43.43	47.69
China	21.4		44.96	46.49	43.43	47.07
Ar-1	10.1		13.43	12.90	12.81	15.47
Ar-2	6.13		6.78	5.77	6.61	6.53
Sa-1	5.21		5.80	6.00	5.36	4.77
Sa-2	2.09		5.00	4.63	4.13	4.22
SI(x100) 0.5IU/ml	0.41		0.62	0.62	0.51	0.49
Negateive	<0.02		<0.07	<0.07	<0.06	<0.06
SI(x25) 2IU/ml	2.00		2.00	2.00	2.00	2.00

Result explanation:

a)There isn't significant difference comparing the detection result of this time with that of before.

b)There still is the significant difference comparing the detection result of WHO Standard Rabies Immunoglobulin and the Chinese Standard Human Rabies Immunoglobulin with their primitive titer.

4) Summarization for the cooperation work in NIID Japan on RFFIT

between the scientists from the two labs, 5-19 Dec 2010

a)Comparing the detection system of RFFIT in the two labs, the Viral Disease Control and Prevention China CDC and the National Institute of Infectious Diseases (NIID) of Japan, it is not completely the same.

b)There exists the difference in RFFIT detection system if it is operated by the different person even in the same lab, because of the operation procedure, microscope observation, titer calculation, different Standard of Rabies Immunoglobulin, and so on.

c)It is necessary that continue the evaluation on RFFIT between the two labs to further adjust the detection system for more stable and relative accuracy. It is needed that to include more cooperation labs to compare the detection system of RFFIT, such as include some of the WHO Collaborating Centers for Reference and Research on Rabies(the Rabies Unit in USA CDC, the National reference centre for rabies in Institute Pasteur), which will be very helpful to improve the RFFIT system not only for China and Japan, but also for the other countries.

YEAR THREE PROJECT REPORT

PROJECT TITLE: ***Search for Lyssaviruses in some bat species in Northern Vietnam.***

NAME OF RESEARCHERS

Dr. Nguyen Thi Kieu Anh, Dr. Nguyen Vinh Dong, Dr. Nguyen Tuyet Thu, Dr. Ngo Chau Giang and Dr. Nguyen Thi Hong Hanh.

AFFILIATION

National Institute of Hygiene and Epidemiology (NIHE), Hanoi, Vietnam.

BACKGROUND

As the results achieved from projects year one and year two which were designed and implemented by NIID and NIHE, the RT- LAMP technique for detection of rabies virus (RABV) was developed and evaluated in terms of its sensitivity and specificity. We found that the detection limit of the prototype RT-LAMP technique developed by our research group reached 2x10 RNA if fixed RABV was used. However, the sensitivity was only 50% when compared with RT-PCR using the samples from rabies suspected patients. Hence, we have continued to find out the optimal condition for the RT-LAMP as well as the most suitable, sensitive primers for detection of wild type strains of RABV isolated in Vietnam.

Up to now, 7 genotypes of the genus *Lyssaviruses* are recognized in the family *Rhabdoviridea* and were reported to cause rabies or rabies like diseases throughout the world. However, in Vietnam as well as in other Asian countries only RABV, genotype 1 of the *Lyssaviruses*, has been recognized and reported. The research on other members of the *Lyssavirus*es both in animal reservoirs and in humans have rarely been carried out. Furthermore, according to the